

Creating and Presenting an Award-Winning Poster

Stephen J. Heishman, Ph.D.
Office of Education and Career Development
NIDA Intramural Research Program



National Institute
on Drug Abuse

Why is a poster better than a talk?

- You totally bomb at giving talks
- Can be viewed while you nap
- Can hang in the department for years
- Cash bar and snacks
- Informal networking

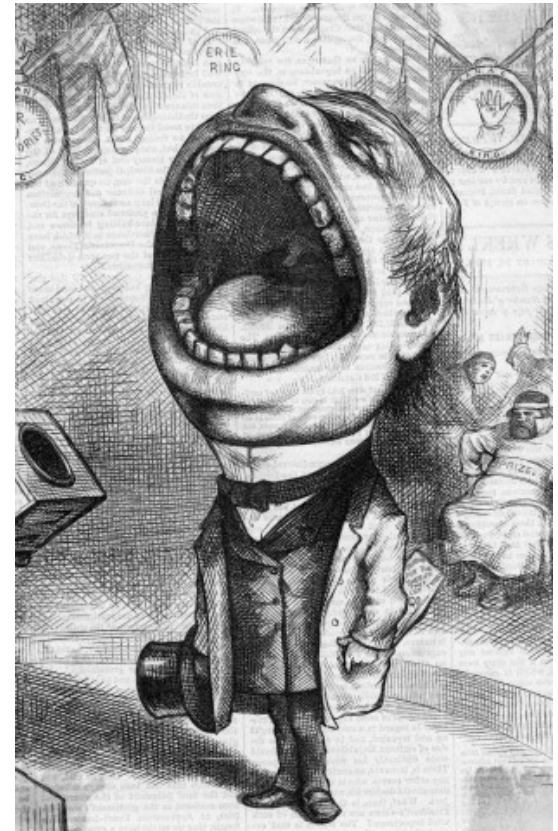
Poster Objectives

- Advertise your science and you
- Receive feedback from mentors & peers
- Develop communication skills
- Build network and contacts
- Use as stepping stone to next level

Creating your poster



Recite after me,
Posters are visual &
less is best!

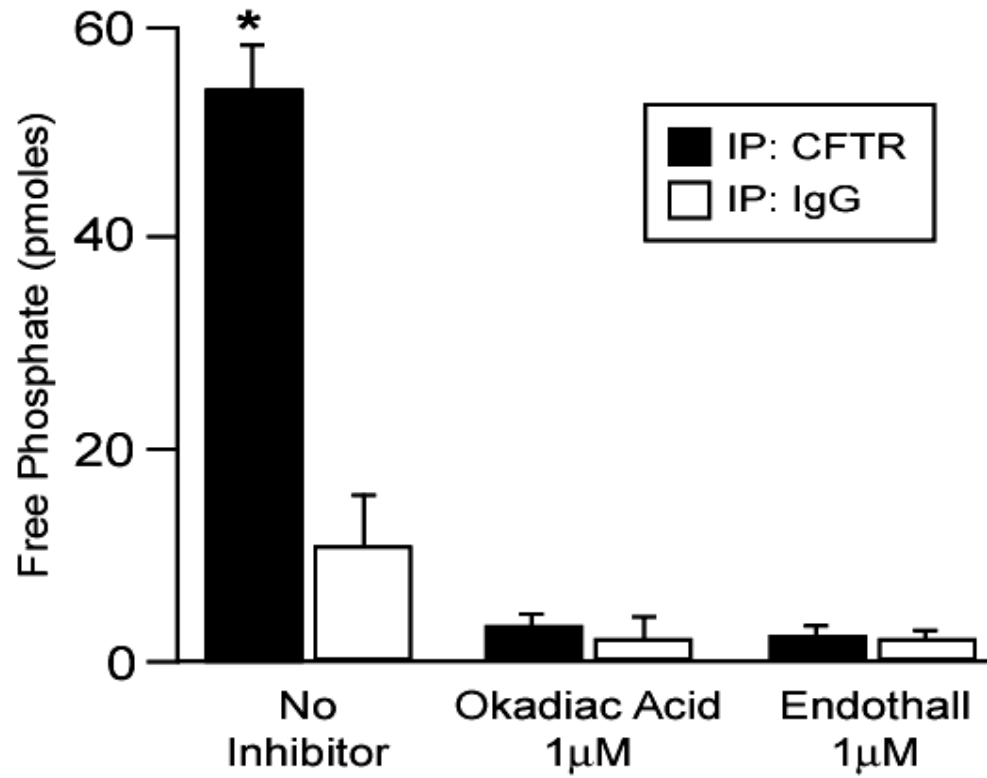


Start with your 2 main elements

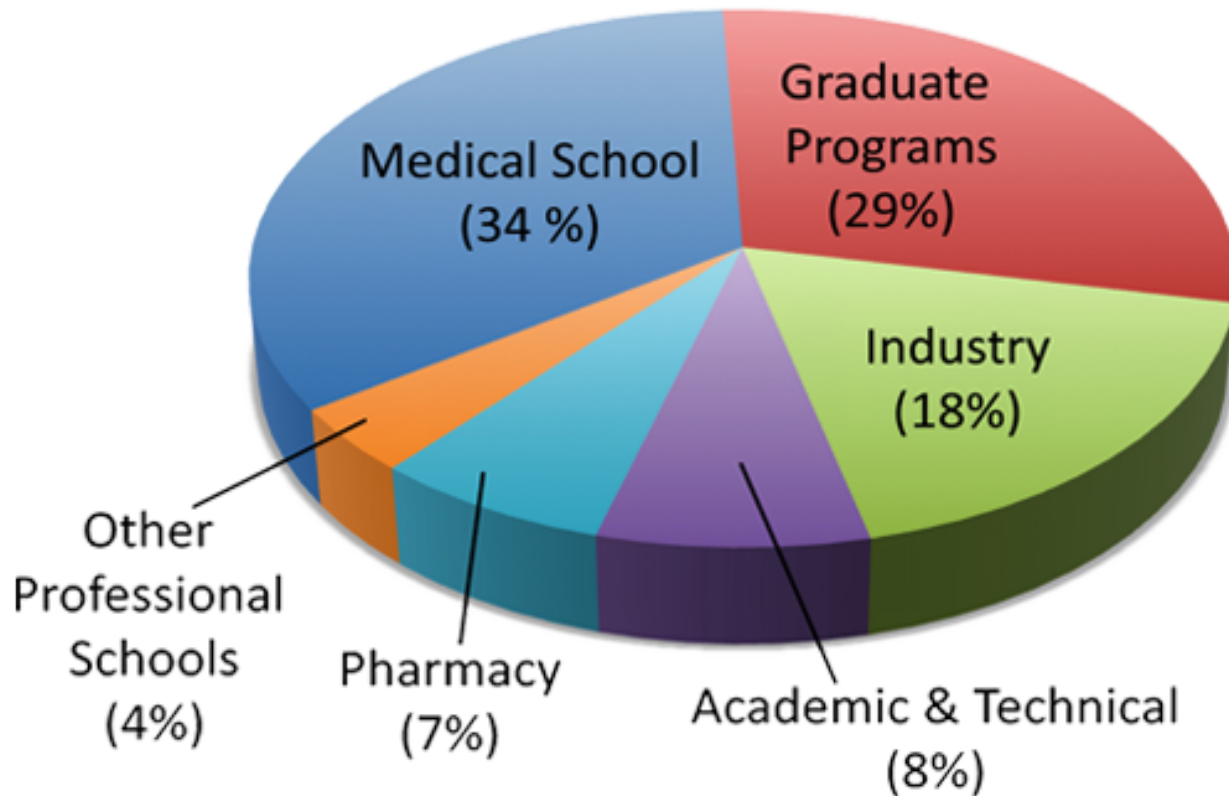
- Simple, effective data displays
- Small blocks of supporting text
- Use these to tell a story

KISS your figures

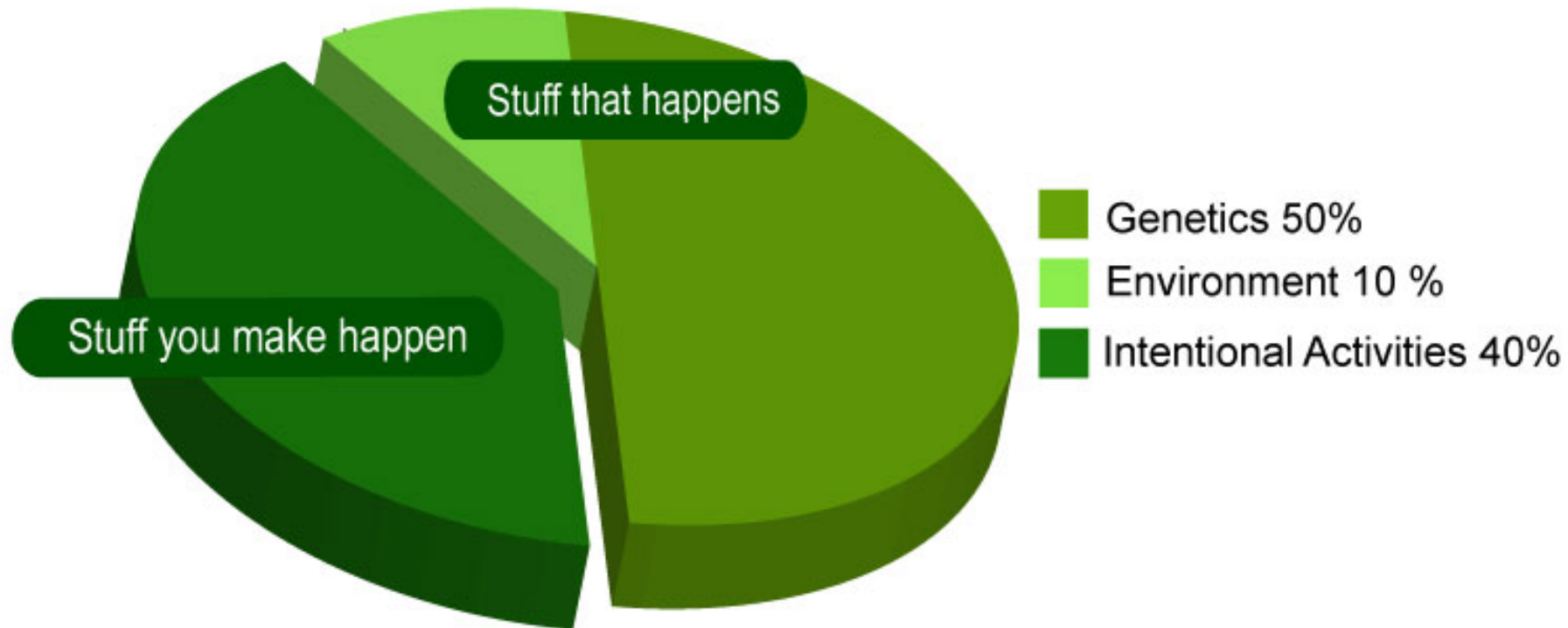
Phosphatase activity assay



Career Paths of Our Graduates



What Determines Your Level of Happiness?



source: Sonja Lyubomirsky's *Pursuing Happiness: The Architecture of Sustainable Change*.
www.faculty.ucr.edu/~sonja/papers/LSS2005.pdf

Figures

- Centerpiece of your poster
- Label axes clearly
- Avoid legends and 3-D graphs
- Put caption with the figure
- Use pictures or photos for Methods

Supporting Text

- Introduction – NO abstract
- Goals/aims/objectives
- Methods
- Results
- Conclusions/Main Findings

Supporting Text

- Font size – think BIG (4-6 feet test)
 - Title 85 pt
 - Headings 36 pt
 - Text > 24 pt (this is 28 pt)
 - Captions > 20 pt
- Use sans-serif font (Helvetica, Arial, Calibri)
- Do NOT use *Comic Sans*

Supporting Text

- Less is best, 50-100 words per element
- Use phrases in bullets
- Left justify
- Use **bold** or **color** or **both** for emphasis

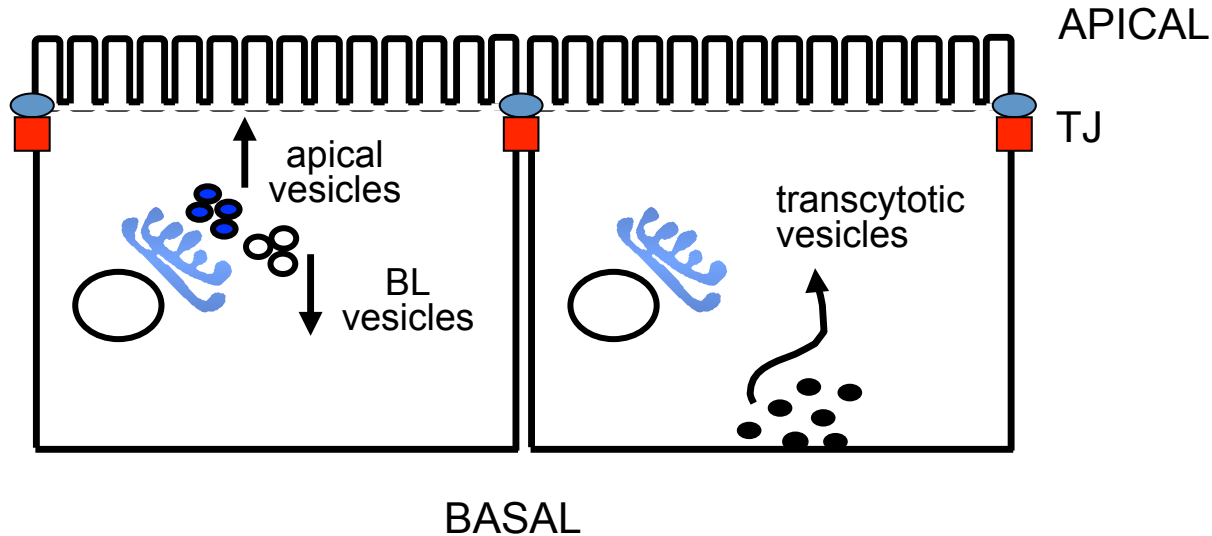
some examples . . .

Before

INTRODUCTION

Epithelial cells are highly polarized with apical, basal and lateral membranes. Tight junctions form a barrier between the apical and basolateral surface. Some proteins are targeted directly to one plasma membrane surface, while some are targeted to the apical membrane following transcytosis from the basolateral surface. We still do not understand the molecular mechanisms that underlie the polarized sorting of proteins in epithelial cells.

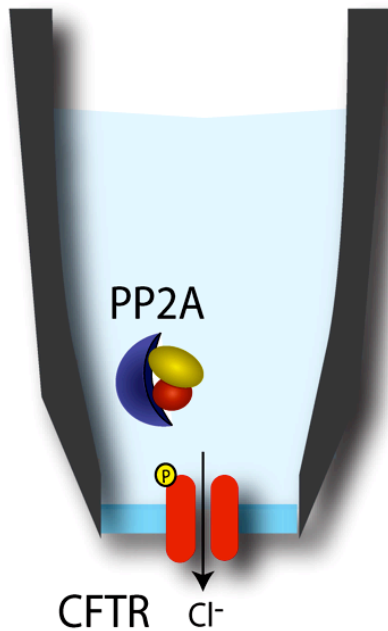
After



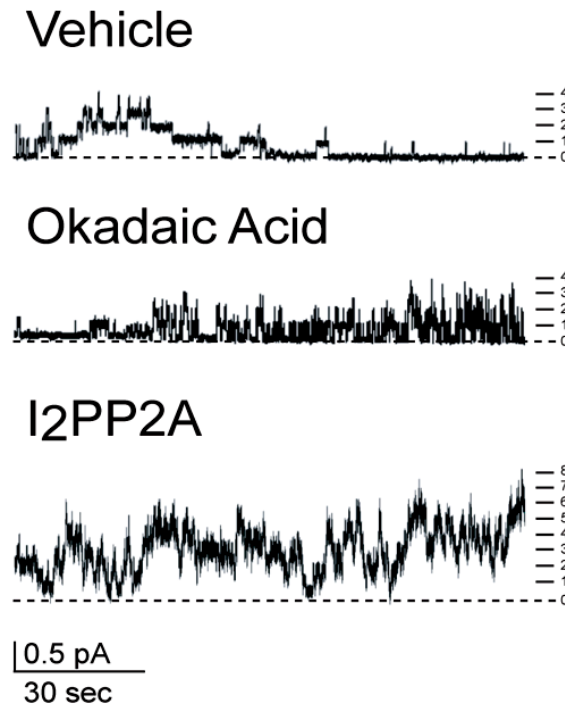
- Epithelial cells are polarized cells with apical, basal and lateral membranes. Tight junctions (TJ) form a barrier between the apical and basolateral surface.
- Some proteins are targeted directly to one plasma membrane surface, while others are targeted to the apical membrane following transcytosis from the basolateral (BL) surface.
- We still do not understand the molecular mechanisms that underlie the polarized sorting of proteins in epithelial cells.

PP2A regulates CFTR channel activity

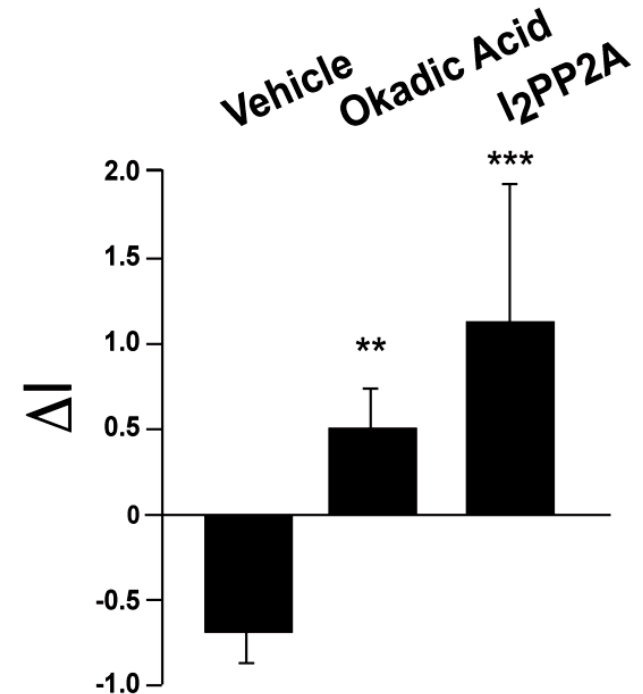
A. Experimental design



B. Single channel recordings



C. Averaged data N=6



Before

Conclusions

We used affinity purification to identify proteins that associate with CFTR and found that the the B' ϵ subunit of PP2A directly associates with the CFTR C-terminus. Using western blotting and in-vitro phosphorylation assays, we showed that PP2A protein and activity co-immunoprecipitate with CFTR from airway epithelial cells. The PP2A B' ϵ is the subunit responsible for targeting the phosphatase to the channel. We further found that PP2A negatively regulates CFTR channel activity in mouse intestinal and human airway epithelial cells. Thus we conclude that inhibitors of PP2A may improve clinical outcomes in cystic fibrosis.

After

Conclusions

- The B' ϵ subunit of PP2A directly associates with the COOH-terminus of CFTR
- PP2A protein and activity co-immunoprecipitates with CFTR in cultured airway epithelial cells
- PP2A negatively regulates CFTR channel activity in mouse intestinal and human airway epithelial cells
- Inhibitors of PP2A may improve clinical outcomes in Cystic Fibrosis

Let's design a poster



Posters are visual

Succinct descriptive title

Authors & affiliations

NIH &
HHS Logos

IC Logo

Introduction

Result 1

Result 4

Goals/Objective

Result 2

**Summary/
Conclusion**

Methods

Result 3

**Other:
Acknowledgements
Contact info**

Poster Layout & Design

- Check poster size & orientation
- Symmetry and balance
- Use white space effectively (20-30%)
- Use colors to engage viewer
 - 2-3 colors, no more
 - white background, not artsy
 - black or dark text

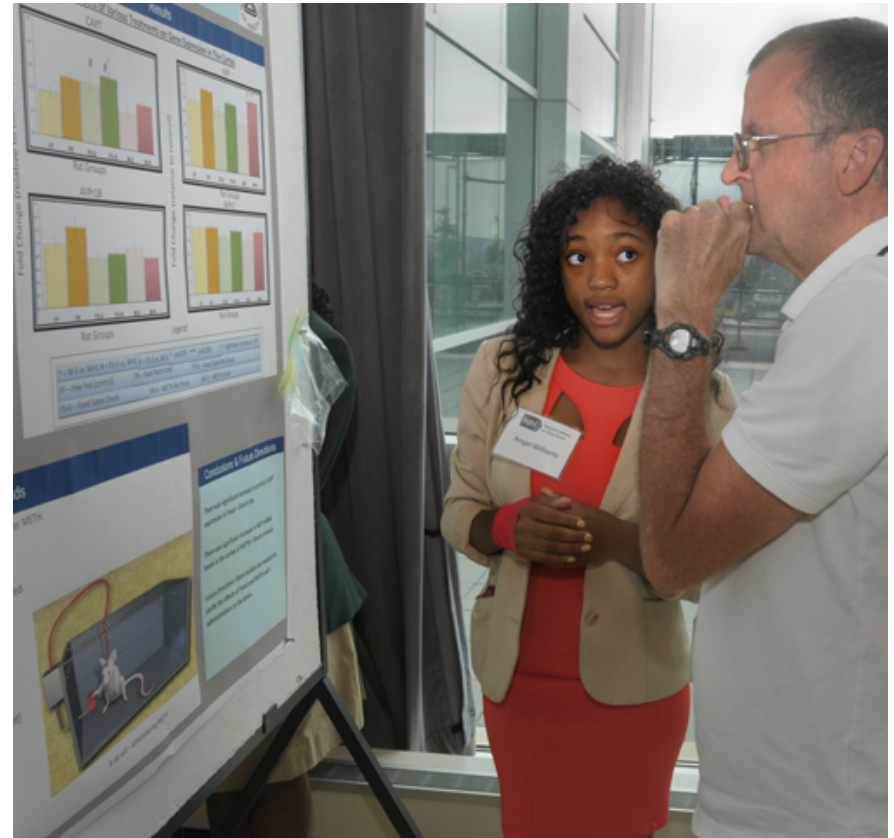
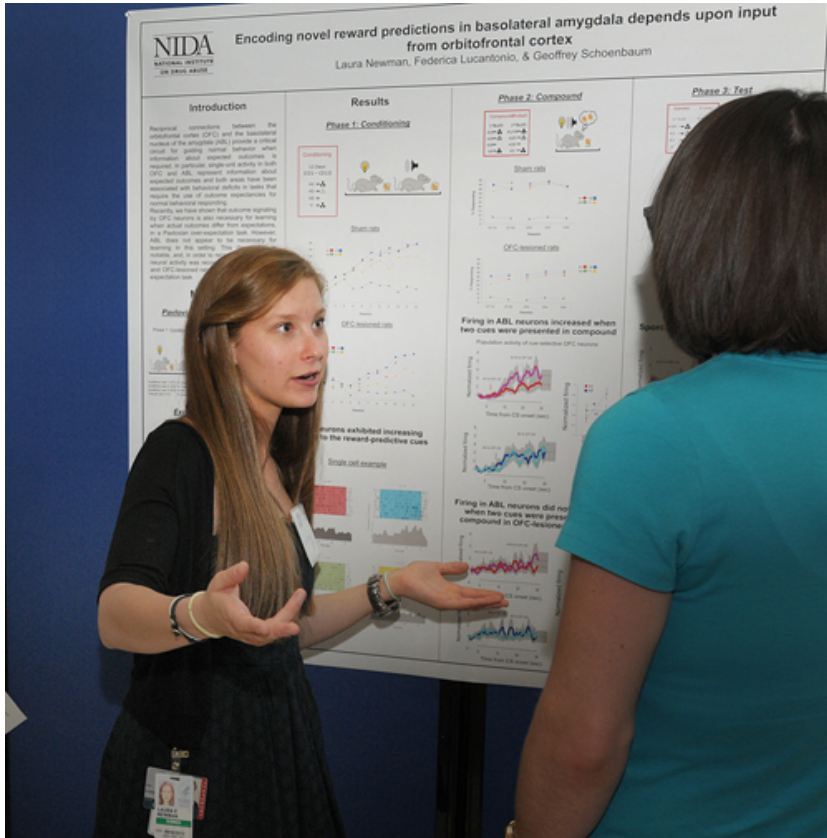
Blue on red appears blurry

Red on blue appears even more blurry

Yellow on white is hard to read

Black on white is best

Presenting your poster



Presentation Pointers

- Prepare a 3-5 min overview
- Practice, practice, practice
- Tell a great story
- Be enthusiastic & maintain eye contact
- Bring mini-poster handouts
- Stay at your poster

Some actual posters . . .

so let's see what you've learned

Free Photoshop PSD file download
Resolution: 1280x1024 px
www.psdgraphics.com



Work Absences and Costs Associated With Rheumatoid Arthritis: A Comparison Between Employees With and Without Rheumatoid Arthritis in a United States Population

Nathan L Kleinman¹, Richard A Brook², Stephanie E Kirbach³, Mary A Cifaldi³

¹Health as Human Capital Foundation, Cheyenne, Wyoming, United States; ²The JestaRx Group, Newfoundland, New Jersey, United States; ³Abbott Laboratories, Abbott Park, Illinois, United States

Abstract

Background/Purpose: Rheumatoid Arthritis (RA) was recently reported to have societal costs in the US of \$19.3 billion and \$39.2 billion (in 2005 dollars) without and with intangible costs, respectively.¹ However, most indirect components were subjectively imputed. This research was designed to use objective data to quantify the incremental work absence and indirect costs associated with RA in an employed population and compare these absences and costs to controls.

Methods: Employee records from multiple large employers in the US providing data about demographic, job-related information, and health care use in the HCMS database were assessed from 1/1/01 to 6/30/10. Patients with RA were identified by claims with primary, secondary, or tertiary ICD-9 codes of 714.xx, and the date of the first claim was considered the index date. Controls were employees without claims for RA, and their index date was defined as the average index date (by employer) among RA patients. All subjects were required to have 12 months continuous health plan enrollment. Absences and indirect costs were measured for the 12 months following each employee's index date. All costs were adjusted to June 2010 US\$. Regression modeling was used to separately compare days absent and indirect costs using 2-part models controlling for demographics, job-related variables, location, and modified Charlson Comorbidity Index.

Results: Out of more than 800,000 employees in the HCMS database, 2705 (0.79% of employees) had RA and 338,035 were controls (Table 1). The incremental indirect costs (RA minus controls, Table 2) were: Sick Leave \$145; Short-term Disability \$249; Long-term Disability \$41 ($P = .0505$); Workers' Compensation \$90; and Total \$525. Incremental absence days (Table 2) were: Sick Leave 1.2; Short-term Disability 1.91; Long-term Disability 0.47 ($P > .05$); Workers' Compensation -0.01 ($P > .05$), and Total 3.58. All comparisons $P < .01$ except where noted. **Conclusion:** Employees with RA incur 71% more indirect costs than those without RA and utilize 82% more lost time.

Background

- Rheumatoid arthritis (RA) has been reported to have societal costs in the United States of \$19.3 billion not including indirect costs (such as quality-of-life deterioration and premature mortality) and \$39.2 billion including indirect costs (values are 2005 US\$)¹
- However, in past analyses, most indirect costs were subjectively imputed using medical claims data to estimate the societal cost of absences from work and using information from literature searches based on published data, jury awards, and life-expectancy estimates to estimate other indirect costs

Objective

- Here, we used objective data collected from an employed population
 - To quantify work absences and indirect costs associated with RA
 - To compare work absences and indirect costs between persons with RA and controls (employees without RA)
 - To estimate the burden of RA in the US civilian labor force

Methods

- Employee records from 1/1/01 to 6/30/10 from multiple large employers in the United States that provided data about demographic, job-related information, and health care use in the Human Capital Management Services (HCMS) database were assessed
- Patients with RA were identified by medical claims with primary, secondary, or tertiary International Statistical Classification of Diseases, 9th Revision, codes of 714.xx. The date of the first claim was considered the index date
- Controls were employees without claims for RA. The index date for controls was defined as the average index date (by employer) for patients with RA
- All patients were required to have 12 months of continuous health plan enrollment after the index date
- Absences and indirect costs for sick leave, short- and long-term disability, and workers' compensation were measured for 12 months following each employee's index date
- All costs were adjusted to June 2010 US\$ using non-seasonally adjusted Consumer Price Indices (CPIs) for medical services, prescription drugs, and all consumer goods²
- Regression modeling was used to compare days absent and indirect costs (separately) using 2-part models that controlled for demographics, job-related variables, geographic location, and modified Charlson comorbidity index (mCCI) score³

- Incremental costs (days) were defined as the costs (days) of the employees with RA minus the costs (days) of the employees in the control cohort
- All statistical analyses were 2-tailed with $\alpha = 0.05$
- To estimate the burden of RA on the population of workers in the United States, the prevalence rate, costs, incremental annual absence costs, and incremental annual absence days determined in this analysis were applied to the US civilian labor force of 139.88 million persons in 2009⁴

Results

- Of the more than 800,000 employees in the HCMS database, 340,740 were eligible for inclusion in the study. Of these, 2705 employees had RA, and 338,035 employees were controls (Table 1)
 - The observed prevalence of RA was 0.794%

Results (continued)

Table 1. Descriptive Statistics For Employees With and Without RA

Variable	Employee With RA (N = 2705)	Employee Without RA (N = 338035)	P-Value
Age at index date (yr), mean (SD)	45.13 (10.06)	40.37 (9.94)	<.0001
Sex, %			
Female	61.4	40.9	<.0001
Male	38.6	59.1	<.0001
Marital status, %			
Married	42.5	45.1	.0095
Not married	31.1	32.9	.0436
Missing	35.4	22.0	<.0001
Race/ethnicity, %			
White, non-Hispanic	44.1	41.3	.0096
Black, non-Hispanic	8.6	11.6	<.0001
Hispanic	10.8	6.6	<.0001
Other single race	2.4	3.6	.0037
Missing	34.1	36.8	.0036
Annual salary, mean (SD)	\$53,400 (\$36,276)	\$53,655 (\$172,919)	.9623
Years of index date (yr), mean (SD)	2.60 (8.73)	8.92 (8.04)	<.0001
Job classification, %			
Exempt	31.3	35.0	.0614
Non-exempt	68.7	65.0	.0614
Work hours, %			
Full-time	94.6	89.7	<.0001
Part-time	5.4	10.3	<.0001
mCCI score, mean (SD)	0.477 (1.106)	0.126 (0.553)	<.0001

*Employees without RA (N = 338,035).

**Employee with RA (N = 2,705); employee without RA (N = 338,035).

- Table 2 presents the indirect adjusted annual costs and the absence days for both cohorts
 - The incremental indirect costs (RA minus controls) per person were
 - Sick leave: \$145
 - Short-term disability: \$249
 - Long-term disability: \$41 ($P = .0505$)
 - Workers' compensation: \$90
 - Total: \$525
 - The incremental work-absence days per person were
 - Sick leave: 1.2 days
 - Short-term disability: 1.91 days
 - Long-term disability: 0.47 days ($P = .1138$)
 - Workers' compensation: -0.01 days ($P = .8715$)
 - Total: 3.58 days
 - All comparisons $P < .01$, except where noted

Table 2. Annual Indirect Costs and Absences For Employees With and Without RA

Component	Employee With RA		Employee Without RA		P-Value		P-Value	
	N	Cost ^a	Days ^b	N	Cost ^a	Days ^b	Cost ^a	Days ^b
Sick leave	1106	\$170	3.25	145,954	\$325	2.05	<.0001	<.0001
Short-term disability	1582	\$469	3.74	188,103	\$218	1.83	<.0001	<.0001
Long-term disability	2153	\$55	0.74	247,407	\$14	0.28	.0905	.1138
Workers' compensation	3440	\$271	0.18	312,226	\$181	0.19	.0093	.8715
Total (sum above)		\$1262	7.92		\$737	4.34		

^aAdjusted mean.

^bDays lost to rounding.

- Table 3 summarizes the projections for the work-absence impact of RA on the US civilian labor force
 - Using the 0.79% RA prevalence rate from the current analysis, the incremental annual indirect costs of \$525/employee, and the work-absence days of 3.58/employee, RA accounted for
 - An annual incremental increase of US\$582.58 million in work-absence costs
 - An annual incremental increase of 4.0 million lost work days (equivalent to more than 15,000 full-time employees)

Table 3. Projections of the Work-Absence Impact of RA on the US Civilian Labor Force

Population Characteristic	US Civilian Labor Force
Base population (million)	139.88
RA prevalence (million, projected)	1.11
Incremental work-absence days (million, projected)	3.58
Incremental annual indirect costs (US\$ million, projected)	\$582.58

Conclusions

- Compared with employees without RA, employees with RA
 - Incur 71% more indirect costs
 - Exhibit 82% more lost time
 - May account for 4 million additional work-absence days annually in the United States

References

- Birbaumer N, et al. *Curr Med Res Opin*. 2010;26:77-80.
- http://data.bls.gov/PDO/tables/jp/turnover. Accessed April 1, 2011.
- Cheskin MC, et al. *J Chronic Dis*. 1987;40:273-83.
- http://www.bls.gov/news.release/emppt01.txt. Accessed August 3, 2011.

Disclosures

NL Kleinman, RA Brook: Consulting Fees: Abbott.
SE Kirbach, MA Cifaldi: Employee & Stockholder: Abbott.

This poster downloaded from <http://jestaRx.com/publications.htm>
Richard Brook (973) 208-8621 RBrook@JeSTARx.com

Presented at the American College of Rheumatology Annual Scientific Meeting, November 4-9, 2011, Chicago, Illinois

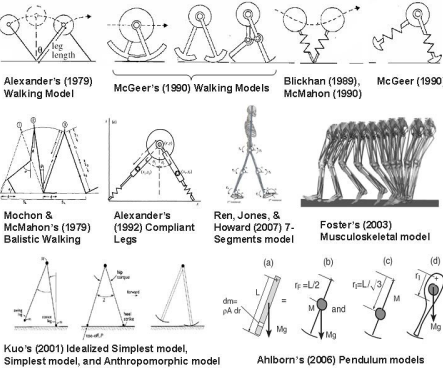
Musculoskeletal Simulation-based Parametric Study of Optimal Gait Frequency in Biped Locomotion

HYPOTHESIS

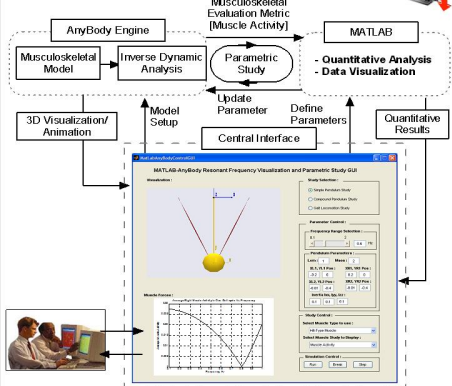
Expanded effort is minimal when the locomotory appendages/ propulsive structures are moving at steady-state in periodic gaits at their resonant frequencies.

MOTIVATION

Obtaining insights that will allow for better design of the robotic systems.
Using virtual computational tools for studying hypotheses regarding locomotory systems.



ANALYSIS FRAMEWORK



Analysis framework: A MATLAB GUI serve as a Center Interface that allows performance studies of walking in response to various inputs. The AnyBody engine provides the computational musculoskeletal modeling while the parametric sweeps and plotting are handled by MATLAB.

CASE STUDIES

- Three case studies:
- (1) Simple Pendulum;
 - (2) Compound Pendulum;
 - (3) 18-DOF Lower Extremity Musculoskeletal Model.
- Both simple and compound pendulum models have been used as a simplified lower extremity model to predict human stride frequency, with some success [2].
- To gain insights to the more complex musculoskeletal model;

Natural Frequency of 'pendulum like' model:

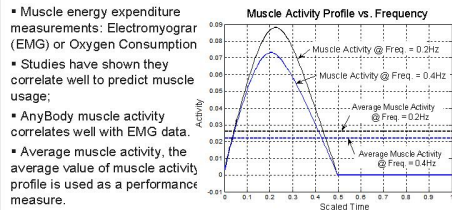
$$\omega = \frac{n}{2\pi} \sqrt{\frac{g}{L}}$$

$n = \sqrt{3}/2 = 1.225$ - Uniform rod;
 $n = \sqrt{5}/2 = 1.581$ - Cone shape;

In previous studies [2], researchers have shown $n = \sqrt{2} = 1.414$ correlates well with the human preferred walking speed;

We compare this with our musculoskeletal simulation results.

Evaluation Metric:

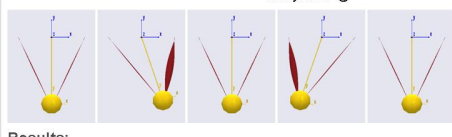
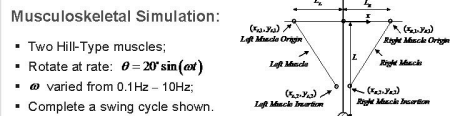


CASE STUDY I - SIMPLE PENDULUM

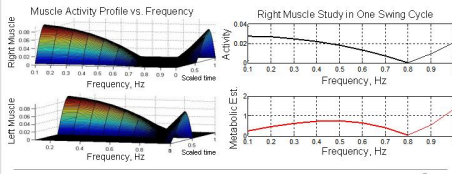
Natural Frequency, ω of Simple Pendulum:

$$\omega = \frac{1}{2\pi} \sqrt{\frac{g}{L_{cm}}}$$

For $L_{cm} = 0.4m$ - distance to center of mass;
 $g = 9.81m/s^2$ - gravitational acceleration;
 $\omega = 0.788Hz$



- Results:
- Muscle activity profile across frequency range 0.1Hz - 10Hz;
 - There appear to have a 'cut-off' frequency where activity is minimum;
 - To locate this minimum, we plot the average muscle activity vs. Freq.;
 - The frequency where minimum muscle activity occurs is 0.79Hz.



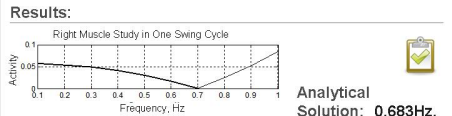
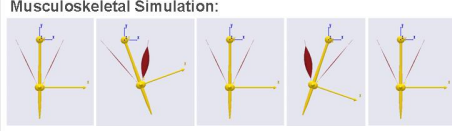
Analytical Solution: 0.788Hz.
Musculoskeletal Simulation: 0.79Hz.

CASE STUDY II - COMPOUND PENDULUM

Natural Frequency, ω of Compound Pendulum (Rod):

$$\omega = \frac{1}{2\pi} \sqrt{\frac{3g}{2L}}$$

For $L = 0.8m$ - length of uniform rod;
 $g = 9.81m/s^2$ - gravitational acceleration;
 $\omega = 0.6825Hz$



Results:

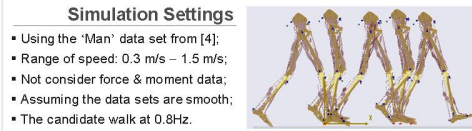
Analytical Solution: 0.683Hz.
Musculoskeletal Simulation: 0.69Hz.

CASE STUDY III - LOWER EXTREMITY

- Human Gait:
- Gait of "Normal Man":
 - Stride Frequency - 0.77Hz
 - Stride Period - 1.3 seconds
 - Stride Length - 1.28 m
 - Speed - 0.99m/s
 - Variance in "natural" walking speed:
 - Village (0.8m/s) vs. Cities (1.7m/s)
 - Long vs. Short walkway
 - Treadmill vs. Natural surfaces
 - Indoor vs. Outdoor
 - 'Walk-run' transition: 1.92m/s

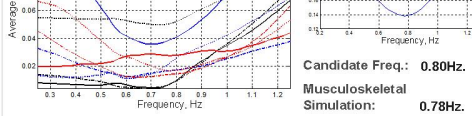
Musculoskeletal Model:

- Available in AnyBody Model Repository [3];
- 7 rigid bodies (Thigh x 2 + Shank x 2 + Foot x 2 + PelVis)
- 27 unique muscles in each leg (54 in total)
- 18 Degree-of-Freedom
- Length: Thigh (0.44m), Shank (0.44m), Foot (0.22m)
- Hill-type muscle model
- Driven by motion capture data (1.25 seconds/cycle)



Simulation Settings

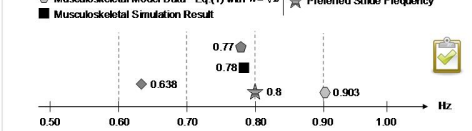
- Using the 'Man' data set from [4];
- Range of speed: 0.3 m/s - 1.5 m/s;
- Not consider force & moment data;
- Assuming the data sets are smooth;
- The candidate walk at 0.8Hz.



Candidate Freq.: 0.80Hz.
Musculoskeletal Simulation: 0.78Hz.

Conclusion:

- The musculoskeletal simulation shows that the system used least effort (minimum activity) at 0.78Hz.
- Closer prediction of the preferred stride frequency (0.80Hz) compare to using equations in [2];
- Potential for use in other what-if-type studies.



REFERENCE

- Lee, L-F, and Krovi, V. "Musculoskeletal Simulation of Optimal Gait Frequency in Biped and Human Locomotion." Proceedings of IEEE ROBOT 2008, Scottsdale, Arizona, October 19-22, 2008.
- K. G. Holt, J. Hamill, and R. O. Andrus, "The Force-Driven Harmonic Oscillator as a Model For Human Locomotion," Human Movement Science, vol. 9, pp. 55-68, 1990.
- AnyBody Technology Group, The AnyScript Model Repository version 6.0, 2006, available for download at: <http://anybody.aau.dk/repository/>.
- C. L. Vaughan, B. L. Davis, and J. C. O'Connor, "Biomechanical Data Resources," Human Kinetics Publishers, 1999.

INTRODUCTION

- Hair analysis done in this study was to detect therapeutic & recreational drugs, including cocaine, opiates, benzodiazepines, PCP, cannabis, & amphetamines
- Hair testing is an acceptable method for long-term assessment of substance-use history
- Hair analysis is used by employers for drug detection & job screening
- Chemical assays of hair are used not only to test for illegal drugs, but also to screen for heavy metals, test for nutritional deficiencies, measure potential toxic & biological chemicals
- Both active drug use & passive drug exposure can result in a positive hair test

Advantages of Hair Analysis:

- Provides longer term information about drug use than urine, blood, or oral fluid¹
- More difficult to adulterate or mask hair than other commonly used drug-screening tests, e.g., urine or blood
- No extensive training required to collect hair samples
- Less invasive collection than other drug tests

Disadvantages of Hair Analysis:

- Hair drug concentrations are low & require sensitive methods of analysis
- Positive readings may not be from drug use but from environmental or passive exposure (e.g., transient smoke in a room)
- No consensus method for hair testing is currently available, so reliability & validity are uncertain
- Surface hair results may not correlate with inner layer hair results
- Cannot do confirmatory repeat analysis if hair sample length is too short¹

Bias:

- Body location of hair sample may yield different results
 - For head hair, most recent drug use is reflected closest to scalp
- Hair color may alter results
 - People with dark colored hair are more likely to have a higher retention of drugs because of higher amounts of melanin in dark hair
 - Color treatment, dye, & washing

History of MDMA (Ecstasy):

- MDMA (3,4-methylenedioxymethamphetamine, or ecstasy) is a schedule I synthetic drug with amphetamine-like & hallucinogenic properties
 - Produces feelings of increased energy, euphoria, emotional warmth, distortions in time, perception, & tactile experiences
- First synthesized in 1912 at Merck
- Became schedule I drug in 1985
 - This prohibited the use of ecstasy as a psycho-therapeutic aid
- Often used at "raves" & other parties

GOALS OF STUDY

- Purpose of Primary Clinical Study (Protocol 04-DA-N394):
 - Quantify MDMA parent drug/metabolite concentrations & examine the pharmacokinetics of MDMA
 - Evaluate how MDMA affects memory, attention, decision making, thinking, & feeling
- Why Use Hair Analysis?
 - Hair analysis provides a longer window of detection than urine or blood
- Goal of This Study:
 - Evaluate agreement between study applicants' self-report & results of hair & urine drug tests

METHODS

Clinical Screening & Hair Analysis:

- Self-report instrument (Drug Use Survey) completed by applicants during initial screening process
 - Ethical considerations require that only individuals with a history of MDMA use be enrolled in a study involving MDMA administration
- Urine & hair samples obtained at the same time during the initial screening process
- Lock of hair (~100 mg) collected on cosmetically unnoticeable portion of head, as close as possible to scalp at posterior vertex
- Hair sample shipped to Psychchemics Corp. (Culver City, CA), where drugs extracted by series of washes, & analyzed by screening radio-immunoassay, followed by confirmatory mass spectroscopy

Data Analysis:

- Self-report categorized as positive if use was within the window of detection for that drug in each test:
 - Urine
 - THC—within prior 14 days
 - Amphetamines—within prior 5 days
 - Hair
 - THC—within prior 4 months, but more than 7 days before sample collection
 - Amphetamines—within prior 4 months, but more than 7 days before sample collection
- Self-report was categorized as negative if subjects reported
 - No use of the drug, or
 - Use outside the window of detection for that test
 - (therefore, 28 MDMA users appear as self-report negative in Tables 2 & 4)
- Demographic characteristics of subjects obtained from study screening, or previously acquired data from prior studies at NIDA (Figs. 1 & 2)
- Percentage of participants who tested positive for a drug = number of participants with positive result divided by total number of samples (Figs. 3 & 4)
- Positive predictive value & sensitivity of urine or hair test use self-report as "gold standard"
- Drug test performance evaluated by a paired χ^2 test for homogeneity (1-tailed, $\alpha = 0.05$)

RESULTS

- 191 subjects provided complete data (self-report, hair & urine samples):
 - 80 MDMA users
 - 111 non-MDMA users
 - 44 cannabis users (drug-using controls)
 - 67 non-drug using controls (controls)
- Majority of subjects were African-American or white men (Figs. 1 & 2)
- About 75% of MDMA users & drug-using controls were cannabimimod positive in urine & hair (Figs. 3 & 4), while <50% of MDMA users tested positive for amphetamines in urine (20%, Fig. 3) or hair (48%, Fig. 4)
- Both hair & urine tests showed good agreement (75-84%) with self-report for cannabis & amphetamines (Tables 1-4)
- All subjects who tested positive for any other amphetamine also tested positive for MDMA (Table 5), suggesting that other amphetamines were present only as metabolites or contaminants
- Urine testing is more sensitive for cannabis (79.3%) than for amphetamines (21.2%) (Tables 1 & 2)
- Urine testing has a higher positive predictive value for cannabis (92.9%) than for amphetamines (64.7%) (Tables 1 & 2)
- Hair analysis for amphetamines had a greater positive predictive value & sensitivity, (77.8% & 53.8%, respectively) than urine test (64.7% & 21.2%, respectively) (Tables 2 & 4)
- Cocaine, opiates, & PCP were found in some urine samples (2.7%) & in some hair samples (5.5%), but numbers were so few that they were omitted from analysis
- Reduced numbers of samples in Tables 3 & 4 is due to some participants having insufficient hair samples to allow testing for THC or amphetamines

Figure 1: Racial Distribution of 191 Study Subjects

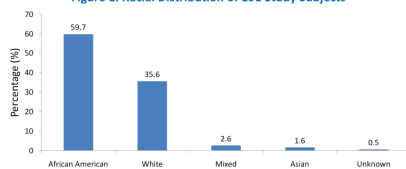


Figure 2: Gender Distribution of 191 Study Subjects by Drug Use Group

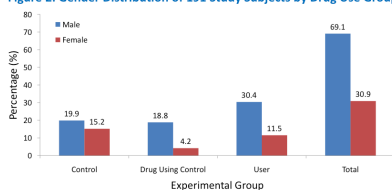


Figure 3: Distribution of Positive Urine Drug Tests by Drug Use Group

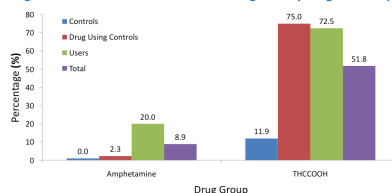


Figure 4: Distribution of Positive Hair Drug Tests by Drug Use Group

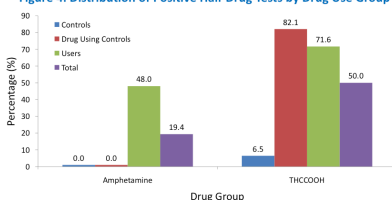


Table 1: 83.8% Agreement between Self-Report & Urine Test for Cannabis*

Urine	Self Report		PPV	92.9%
	Positive	Negative		
Positive	48.2% (92)	3.7% (7)	Sensitivity	79.3%
Negative	12.6% (24)	35.6% (68)		

$\chi^2 = 8.3 \quad p = 0.004$

PPV = positive predictive value

* Data presented as % (n) of total sample (N = 191)

Table 2: 75.4% Agreement between Self-Report & Urine Test for Amphetamines*

Urine	Self Report		PPV	64.7%
	Positive	Negative		
Positive	5.8% (11)	3.1% (6)	Sensitivity	21.2%
Negative	21.5% (41)	69.6% (133)		

$\chi^2 = 24.6 \quad p = 7.07E-07$

PPV = positive predictive value

* Data presented as % (n) of total sample (N = 191)

Table 3: 81.0% Agreement between Self-Report & Hair Analysis Test for Cannabis*

Hair	Self Report		PPV	90.5%
	Positive	Negative		
Positive	45.2% (76)	4.8% (8)	Sensitivity	76.0%
Negative	14.3% (24)	35.7% (60)		

$\chi^2 = 7.0 \quad p = 0.008$

PPV = positive predictive value

* Data presented as % (n) of total sample (N = 168)

Table 4: 82.8% Agreement between Self-Report & Hair Analysis Test for Amphetamines*

Hair	Self Report		PPV	77.8%
	Positive	Negative		
Positive	15.1% (28)	4.3% (8)	Sensitivity	53.8%
Negative	12.9% (24)	67.7% (126)		

$\chi^2 = 7.0 \quad p = 0.008$

PPV = positive predictive value

* Data presented as % (n) of total sample (N = 186)

Table 5: Number of Users Who Tested Positive for Various Amphetamines in Hair

Number of Participants	Tested Positive For MDMA
36	MDMA only
15	MDMA, Amphetamines
1	MDMA, Amphetamines, Methamphetamine
2	MDMA, MDA
7	MDMA, MDA, Amphetamines
1	MDMA, MDA, Amphetamines, Methamphetamine
2	MDMA, MDA, Amphetamines, Methamphetamine
1	MDMA, MDA, Methamphetamine
7	MDMA, Methamphetamine

DISCUSSION

- Demographic characteristics of our sample reflect those of the Baltimore metropolitan area, from which most of the subjects were recruited (other areas include: Washington D.C., Philadelphia, & Annapolis)
- Almost three-quarters of MDMA users also used cannabis, suggesting that pure MDMA use is not common
- >80% percent of participants have self-reports for drug use consistent with test results, suggesting self-reports are accurate
- Major limitation of this study is use of self-report as the "gold standard" for drug use in evaluating hair & urine drug testing. However, in the context of this non-treatment research study, there were no adverse consequences for accurately reporting drug use, a factor known to promote accurate self-report. Participants may lack accurate knowledge of their street drug use or have misunderstood the Drug Use Survey.

CONCLUSIONS

- Hair analysis is more sensitive than a urine test in detecting amphetamines
- However, hair analysis may not be useful for MDMA because false negatives are greater than true positives, i.e., the test has low overall sensitivity compared to self-report

ACKNOWLEDGEMENTS

This research was supported by the Intramural Research Program of the NIH, National Institute on Drug Abuse. John Etter, Janeen Nichols, & Dan Lipstein helped gather & compile data; Matthew Market helped with the statistical analysis.

References:

*Cooper GAA, Allen DL, Scott KS, Oliver JS, Ditton J, Smith ID. Hair Analysis: self-reported use of "speed" & "ecstasy" compared with laboratory findings. J Forensic Sci 2000, 45 (2): 400-406

Targeting Human Disease with Virus Mimicry

Nicholas Francella,¹ Mathias Viard,^{1,3} Anu Puri,¹ Robert Blumenthal,¹ and Amy Jacobs^{1,2}

¹Center for Cancer Research Nanobiology Program, National Cancer Institute at Frederick, National Institutes of Health, Frederick, MD

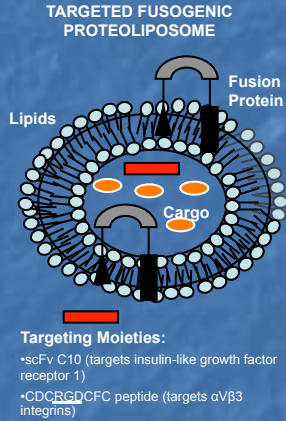
²Department of Microbiology and Immunology, School of Medicine and Biomedical Sciences, State University of New York (SUNY) at Buffalo, Buffalo, NY

³SAIC-Frederick, Inc., NCI-Frederick, Frederick, MD

Abstract

Viruses hijack human cells using a variety of sophisticated mechanisms that range from fusion with the cell membrane to regulation of protein expression and genetic modification. These natural principles are excellent models from which we can design targeted therapies to treat human disease.

We are designing nanoparticles that are based upon virus entry mechanisms. One of our hypotheses is that the efficiency of nanoparticle payload delivery can be dramatically enhanced by the capacity for direct membrane fusion with the plasma membrane. We are utilizing viral membrane fusion proteins incorporated into liposomal nanoparticles to deliver payloads directly into the cytoplasm of targeted cells.



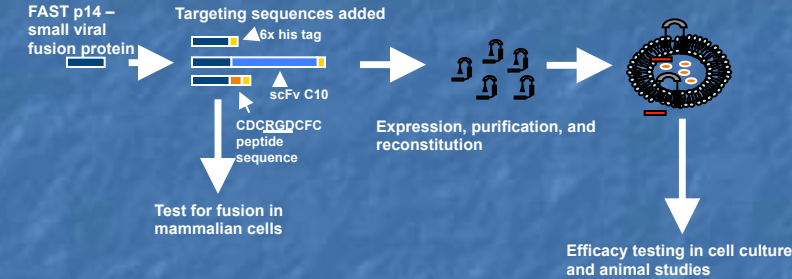
Introduction

The great promise of **nanoparticle delivery** is its ability to salvage drugs or other therapy modalities that have successfully made it far into preclinical or clinical trials, but that have failed near the end of the pipeline because of toxicity or deleterious immunological response.

Liposomes present a promising biomaterial-based method of therapeutic delivery, constituting more than 250 NIH clinical trials.¹ A primary issue that remains unresolved in liposomal delivery, and in nanoparticle delivery in general, is avoidance of the endocytic pathway, which often leads to uncontrolled release, sequestering, and/or degradation of cargo molecules in vesicles in the entry pathway.

Our goal is to avoid the endocytic pathway by direct fusion with the plasma membrane. The fusogenic protein that we use is a fusion-associated small transmembrane (FAST) protein, p14, from a reptilian reovirus.² FAST p14 is promising in engineering fusogenic liposomes because it is much smaller, at 14 kDa, and less complex than other fusogenic protein machinery, for instance, the HIV-entry machinery, which is a trimer of heterodimers at ~500 kDa.

Methodology



Results

Fig. 1: FAST p14 chimeras containing C-terminal targeting peptides retain fusogenic activity.

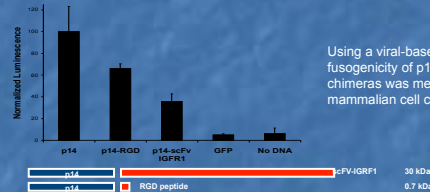
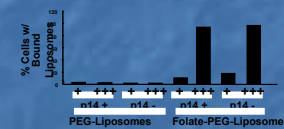
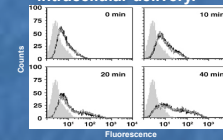


Fig. 2: FAST p14 liposomes can be targeted to specific cell receptors.



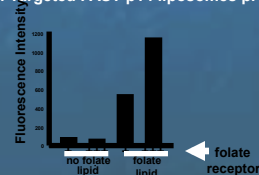
Treatment of cells to up-regulate the folate receptor resulted in a dramatic increase in liposome adherence to target cells.

Fig. 3: FAST p14 liposomes promote fusion and intracellular delivery.



The increased fluorescence in cells seen by the rightward shift in fluorescence, indicates that calcein entrapped in the liposomes, self-quenching at higher concentrations, has been released into the cytoplasm.

Fig. 4: Targeted FAST p14 liposomes promote increased intracellular delivery.



Cell fluorescence increase caused by folate-targeted liposomal delivery was quantified, correcting for the background fluorescence at the non-fusogenic temperature of 4°C.

Conclusions

- FAST p14 remains fusogenic with the addition of targeting moieties to the C-terminus of the protein.
- FAST p14 does not interfere with targeting of liposomes to cells using a folate lipid targeting the folate receptor.
- Targeted-FAST p14 liposomes show increased intracellular delivery.

Ongoing Work

- Test RGD and scFv-chimeras for targeted fusion with cells
- Encapsulate and deliver cytotoxic drugs
- Encapsulate and deliver pro-apoptotic peptides
- Deliver DNA/RNA
- Begin testing in small animal models

Future plan

Pursue detailed studies of virus mechanisms with an eye toward utilization of this knowledge to drive innovation in nanomedicine.



References

1. Information on Clinical Trials. *National Library of Medicine*. www.clinicaltrials.gov.
2. Top, D, R de Antueno, J Salsman, J Corcoran, J Mader, D Hoskin, A Touhami, MH Jericho, R Duncan (2005). *EMBO J*. 24: 2980-2988.

Collaborators

Roy Duncan, Faculty of Medicine, Department of Microbiology and Immunology, Dalhousie University, Nova Scotia, Canada

Jacek Capala, Radiation Oncology Branch, National Cancer Institute, Bethesda, MD

Dimitar Dimitrov, Center for Cancer Research Nanobiology Program, NCI-Frederick, Frederick, MD

Somatic journey to pluripotency and back to lineage commitment

Anna Davidhi¹, Marta Wegorzewska², Rafael Casellas², Lisa Boyette³, Rocky Tuan³, Eran Meshorer⁴, Itai Tzchori¹, Heiner Westphal¹

¹Laboratory of Mammalian Genes and Development, National Institutes of Health, Bethesda, Maryland 20892, USA. ²Genomic Integrity and Immunity, National Institute of Arthritis and Musculoskeletal and Skin Diseases, National Cancer Institute, National Institutes of Health, Bethesda, MD 20892, USA. ³Cartilage Biology and Orthopaedics Branch, National Institute of Arthritis and Musculoskeletal and Skin Diseases, National Institutes of Health, Bethesda, MD 20892, USA. ⁴Department of Genetics, Institute of Life Sciences, The Hebrew University of Jerusalem, Jerusalem, 91904, Israel.

Background

Somatic cell reprogramming reverts the epigenetic and subsequently the differentiation identity of a cell to a pluripotent embryonic stem cell-like state. Embryonic stem cells (ESC), obtained from the inner cell mass of the blastocyst, are pluripotent; they are unspecialized, possess long term renewal ability and can give rise to the whole embryo excluding the extraembryonic tissue. As such they are highly prized for patient specific tissue replacement. The birth of Dolly in 1997, by somatic cell nuclear transfer, showed that cellular differentiation is a reversible process when germ line modifications are not involved. Thus, in the presence of the appropriate "reprogramming environment" the epigenetic memory of a cell is re-established to a pluripotent-like state. A somatic cell becomes pluripotent-like when fused with an ESC either by polyethylene glycol (PEG) or by electrofusion. In 2006, Yamanaka *et al.* showed that this "reprogramming environment" can also consist of four retrovirally encapsulated transcription factor genes, which when transfected into somatic cells give rise to **induced pluripotent stem (iPS) cells**.



Dolly the sheep

All these three reprogramming methods employ major architectural changes in genome expression patterns including histone post-translational modifications. These biochemical alterations work combinatorially and cumulatively in defining the pluripotent state of a cell and thereby its biological function.

Objective

- We have employed two strategies to investigate interrelated factors influencing somatic cell reprogramming:
- **Baculovirus mediated fusion** of two ESC lines with mouse embryonic fibroblasts (MEFs) investigating:
 1. Is the reprogramming ability of different ESC lines, as measured by the overall number of tetraploid hybrids obtained, "the same"?
 2. Are chromatin remodeling markers involved in modulating this phenotype and if so how?
 - **Viral mediated transfection** of MEFs addressing the questions:
 1. Is the iPS reprogramming ability any different from that of a standard ESC? If so, is this ability amenable to pharmacological manipulation?
 2. Can iPS in vitro differentiate well into the Mesenchymal Stem Cell (MSC) lineage and then into mesodermal tissue?

Materials and Methods

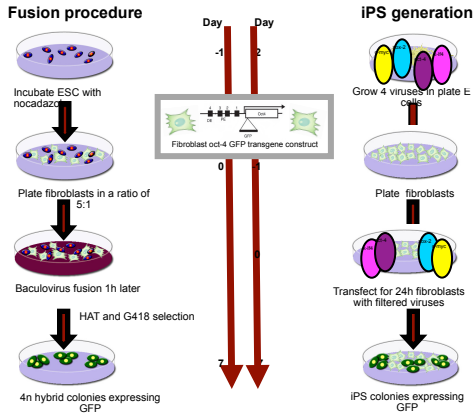


Figure 1. Flow chart of reprogramming by baculovirus mediated cell fusion (left panel) and by retroviral transfection of 4 genes (right panel).

The MEF/ESC hybrid possesses pluripotent-like properties

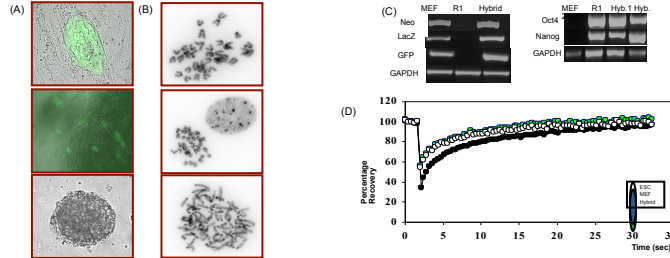


Figure 2. (A) From top to bottom, oct4-GFP expressing hybrid colony, has the ability to self-renew, as well as form in vitro embryoid bodies. (B) From top to bottom, karyotype analysis of 2n ESC nucleus, 2n fibroblast nucleus, and 4n MEF/ESC hybrid nucleus. (C) Left panel: Genotype of MEF, R1 and hybrid for transgene markers. Right panel: Gene expression analysis by reverse transcription-polymerase chain reaction. Lane 1: MEF; Lane 2: R1 ESC; Lane 3 and 4 MEF/ESC hybrid and hybrid2. (D) Pluripotency assay properties of MEF/ESC hybrid chromatin. Fluorescence recovery after photobleaching of CFP labeled heterochromatin protein 1 (HP1) in wild type ESC (white circles), MEF (black circles) and MEF/ESC hybrid (green circle).

Increased H3K9 acetylation levels elevate stem cell potency

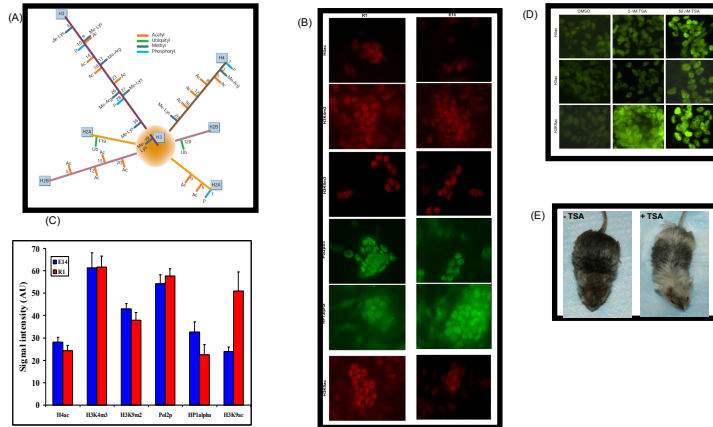


Figure 3. (A) Chromatin histone modifications Adapted from Felsenfeld and Groudine (2003). (B) Immunofluorescent images of pan-acetylated H4 (H4ac), tri-methylated H3 on lysine 4 and 9 (H3K9me3), RNA polymerase II phosphorylated on serine 5 (Pol2pS5), H3K9me3 and H3 acetylated at lysine 9 (H3K9ac). (C) Quantification of B. The Y axes contains arbitrary fluorescent units. Values represent results from at least 20 cells from 3 independent experiments. (D) TSA treatment increases H3K9ac in the E14 stem cell line. E14 cells are treated with the vehicle (DMSO, left), 5nM (middle), and 25nM (right) of trichostatin A (TSA). Immunofluorescence of histone acetylation levels were done by using antibodies specific for pan-acetylated H4 (H4ac, top), pan-acetylated H3 (H3ac, middle) and H3 acetylated on lysine 9 (H3K9ac, bottom). (E) From left to right E14 chimera mice without TSA treatment and with 24h TSA treatment.

iPS derived from MEF's differentiate into mesodermal lineages

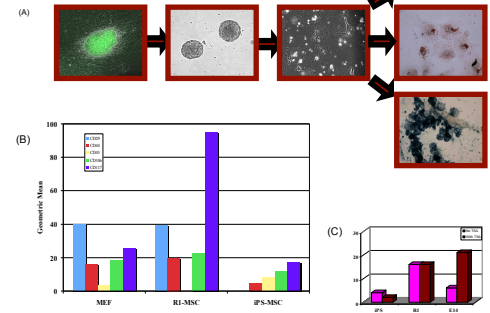


Figure 4. (A) From left to right: Fluorescence microscopy of an iPS GFP expressing colony, phase contrast microscopy of iPS-derived embryoid bodies, phase contrast microscopy of iPS-derived MSCs. From top to bottom: alkaline red staining of MSC derived osteocytes, oil red staining of MSC derived adipocytes and alkaline phosphatase staining of MSC derived osteocytes. (B) Comparison of cellular differentiation marker expression levels for different cell types as measured by flow cytometry. (C) Comparing the reprogramming abilities of iPS, R1 and E14 stem cell lines with and without TSA treatment. The Y axes represents the number of MEF/ESC hybrids obtained for 20 million ESC used.

Conclusions

- Reprogrammed hybrids exhibit pluripotent like characteristics such as morphology, long term renewal ability, embryoid body formation, gene expression profile and chromatin protein hyperdynamic plasticity.
- Different ESC lines display characteristic higher-order chromatin structure. While it is true that no one singular epigenetic modification invariably translates to one single biological output, we have shown that pharmacologically elevated levels of H3K9ac significantly increase the overall reprogramming ability of the E14 ESC line as measured by the most stringent reprogramming criterion: chimera contribution.
- When iPS are fused again with somatic cells from which they themselves originated, they reprogram them, although the efficiencies of this reprogramming merit further investigation.
- iPS differentiate into MSC's but flow cytometry analysis indicates that there are significant differences in the cellular differentiation marker levels as compared to standard in vitro ESCs.

Future Direction

- iPS are heterogeneous with respect to pluripotency. In attempts to "quantify" such stemness differences we will investigate arbitrary H3K9ac chromatin epigenetic remodeling.
- The in vivo aspect of our work, will focus on examining the functional potential of iPS derived differentiated cells.
- Present iPS generating methods are such that these "golden cells" are still disqualified for translational use due to their increased oncogenic potential. We are working on finding methods to efficiently generate clinically usable iPS.

References

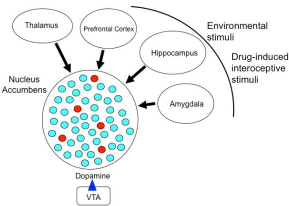
1. Cowan CA, Allentez J, Melton DA, Eggan K. Nuclear reprogramming of somatic cells after fusion with human embryonic stem cells. *Science* 309, 1369-1373 (2005).
2. Hoshikawa Y, Kwon HJ, Yoshida M, Horinouchi S and Beppu T. Trichostatin A induces morphological changes and gelatin expression by inhibiting histone deacetylase in human carcinoma cells. *Experimental cell research* 214, 189-197 (1994).
3. Meshorer E, Yelajala D, George E, Scambler PJ, Brown DT and Mitali T. Hyperdynamic plasticity of chromatin proteins in pluripotent embryonic stem cells. *Development* Cell 10, 105-116 (2006).
4. Takahashi K, & Yamanaka S. Induction of pluripotent stem cells from mouse embryonic and adult fibroblast cultures by defined factors. *Cell* 126, 663-676 (2006).

Mechanism of Daunomycin-Induced Neuronal Inactivation: Caspase-3

Vani Selvam, Shannon Adams, Eisuke Koya, Bruce Hope
Behavioral Neuroscience Branch, NIDA/IRP/NIH/DHHS, Baltimore, MD

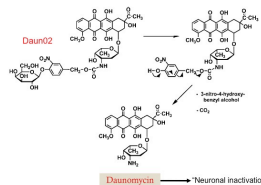
Introduction:

Drug addicts develop learned associations between the drug and the environment where drug is taken. Learned associations are thought to be encoded within sparsely distributed patterns of neurons called neuronal ensembles.



The transformation of Daun02 to its active form daunomycin has been used for targeted disruption of neuronal ensembles activated by drug-related behaviors

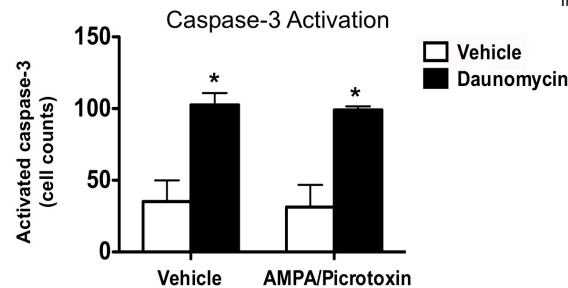
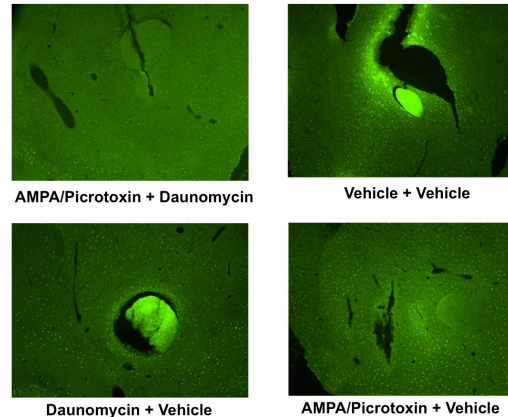
β -galactosidase activates the prodrug Daun02



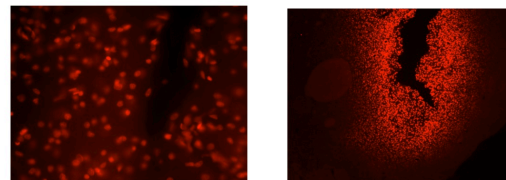
Objective:

The focus of this experiment was to test whether daunomycin will inhibit AMPA-picrotoxin's ability to activate neurons by inducing apoptotic cell death. This will be assessed by the expression of activated caspase-3, an apoptosis-related cysteine protease.

Results:



Results for Daunomycin vs Vehicle are statistically significant ($p < 0.0001$)



Daunomycin injection site (colored red) at 400X (left) and 100X (right)

Methods:

Intracranial Surgery

- Anesthetize rats with Equithesin
- Shave surgical area and clean with ethanol and Betadine scrub
- Place rat in stereotaxic ear bars, cut surgical area, and determine coordinates relative to Bregma.
- Drill hole in skull and insert Hamilton syringe with tip in core of nucleus accumbens.
- Inject 0.5 μ l of combinations of AMPA/picrotoxin (or vehicle) and daunomycin (or vehicle).

	Group A CONTROL	Group B TEST
Left Side Brain	Vehicle / Vehicle	AMPA-picrotoxin / Vehicle
Right Side Brain	Vehicle / Daunomycin	AMPA-picrotoxin / Daunomycin

- Perfuse the rats with paraformaldehyde and extract brains.

Immunofluorescence:

- Slice brains 30 μ m thick and prepare free floating sections
- Permeabilize 20 mins in TBS+Triton X-100
- Place sections in 1 mL of 1:250 concentration of cleaved caspase-3 primary antibody (Cell Signaling) diluted into TBS Triton X-100
- Shake overnight at 4 degrees Celsius
- Place sections in 1 mL of 1:200 concentration of secondary antibody (Anti-rabbit Alexa 488 from Invitrogen diluted into TBS+Triton X-100).
- Mount sections onto glass slides, cover slip, and observe under the microscope

Conclusions:

- Daunomycin induces apoptosis as indicated by significant activation of caspase-3.
- AMPA/picrotoxin does not have an effect on caspase-3

Introduction

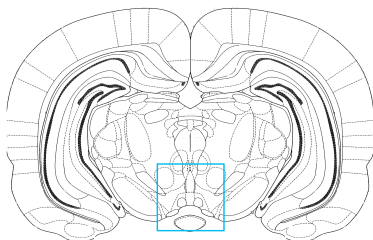
The Ventral Tegmental Area (VTA) is involved in reward and motivation. It contains at least four types of neurons: dopaminergic (containing tyrosine hydroxylase, TH); GABAergic (containing glutamic acid decarboxylase, GAD); glutamatergic (containing vesicular glutamate transporter type 2 VGluT2); and neurons that coexpress both TH and VGluT2. However, the specific distribution and relative proportions of these neurons within the VTA and adjacent midline nuclei remain unknown.

Aims

- To investigate the ratios of dopaminergic, GABAergic, and glutamatergic neurons relative to one another within the VTA
- To investigate how these different phenotypes of neurons are distributed within the VTA

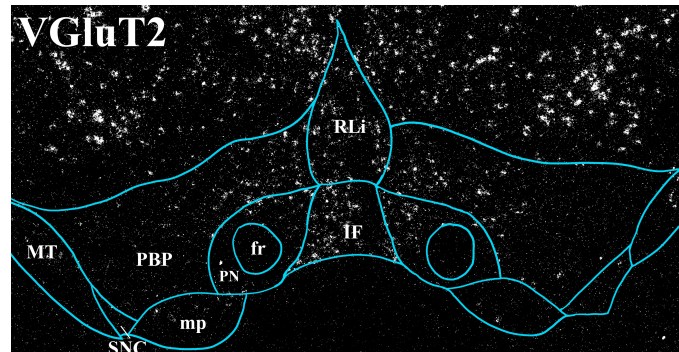
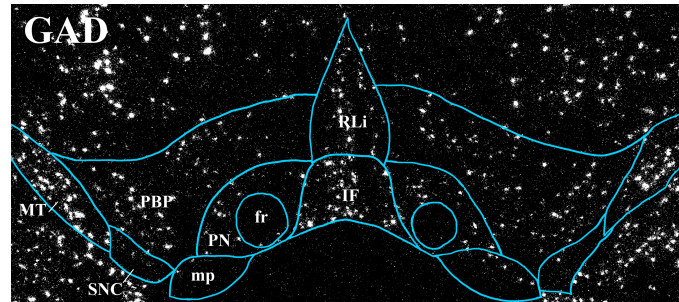
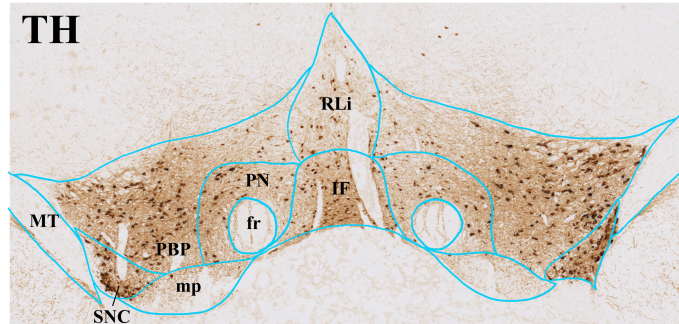
Materials & Methods

- Adult Sprague-Dawley male rats were perfused with 4% paraformaldehyde
- Sections from the VTA were prepared – 5µm thick
- Sequential sections were divided into two groups and hybridized with either VGluT2 or GAD antisense radioactive riboprobes
- All sections were immunostained for detection of TH



This image shows the entire rat brain at Bregma -5.28 (mm) (Paxinos and Watson, 2007).

Distribution of Dopaminergic (TH), GABAergic (GAD), and Glutamatergic (VGluT2) Neurons

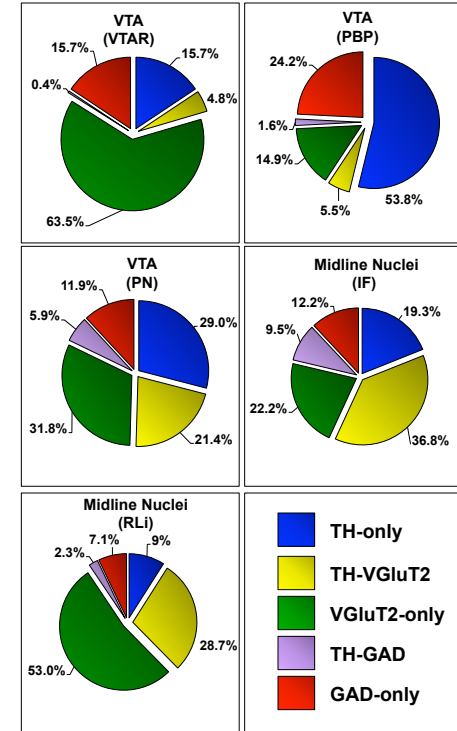


VTA: -ventral tegmental rostral area (VTAR)
-parabrachial pigmented nucleus (PBP)
-paranigral nucleus (PN)

Midline Nuclei: -rostral linear nucleus (RLi)
-interfascicular nucleus (IF)

Summary

Five Different Phenotypes of Neurons are Present in the VTA and Adjacent Midline Nuclei:



Conclusions

- Dopaminergic, GABAergic and glutamatergic neurons are distributed differently throughout all subdivisions of the VTA and adjacent midline nuclei
- A subpopulation of dopaminergic neurons in the VTA and adjacent midline nuclei coexpress a glutamatergic phenotype
- A subpopulation of dopaminergic neurons in the VTA and adjacent midline nuclei coexpress a GABAergic phenotype

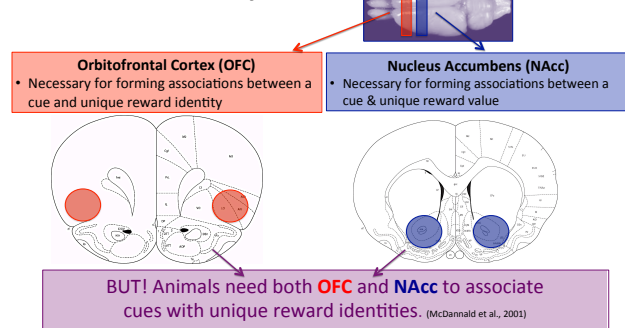
Are OFC-activated NAcc neurons necessary for value discrimination?

A Noreuil, B Berg, TA Stalnaker, and G Schoenbaum

Cellular Neurobiology Research Branch, National Institute on Drug Abuse, National Institutes of Health, Baltimore MD

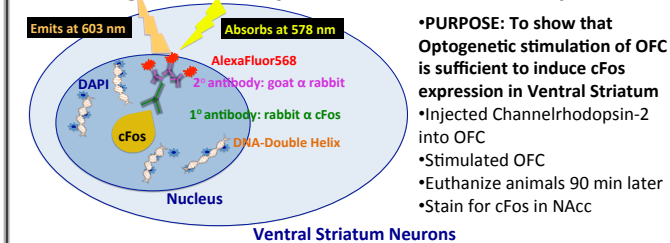


OFC to NAcc Pathway:

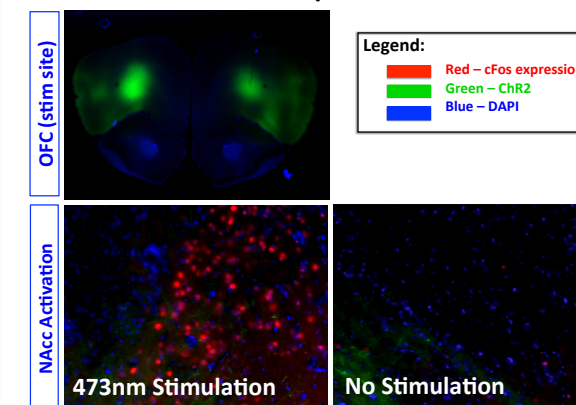


Hypothesis: The NAcc cell population stimulated by OFC is necessary for associating cues with change in reward value and identity.

Validating Methods by Immunohistochemistry

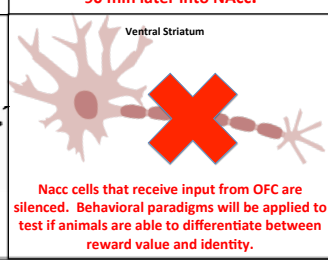
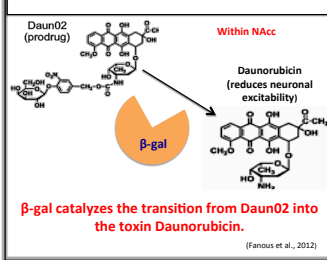
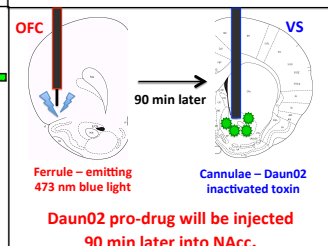
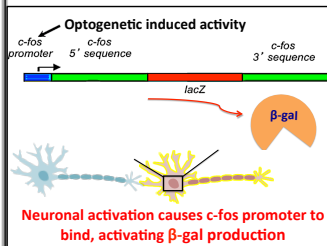
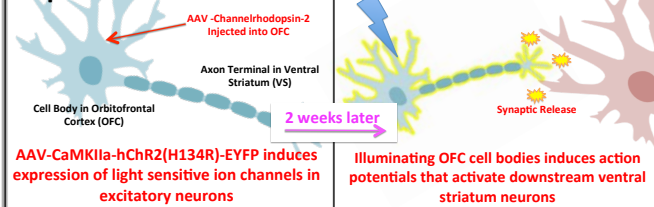


OFC Stim Induces cFos Expression in NAcc:



- OFC injections were on-target
- Laser stimulation induced cFos expression in NAcc
 - Control 1) No stimulation
 - Control 2) eYFP virus

Experimental Outline:



Future Plans:

- Use c-fos-LacZ transgenic rats
- Induce cFos expression in NAcc using optogenetic stim of OFC
- Silence cFos expressing cells using Daun02
- Conduct behavioral tests to determine if NAcc cells that receive OFC input are necessary for learning about changes in reward value

References:

McDannald, Michael A., and Federica Lucantoni. "Ventral Striatum and Orbitofrontal Cortex Are Both Required for Model-Based, But Not Model-Free, Reinforcement Learning." *The Journal of Neuroscience* 31.7 (2011): n. pag. Print.

Fanous, Sanya, Evan M. Goldart, and Florence R. Theberge. "Role of Orbitofrontal Cortex Neuronal Ensembles in the Expression of Incubation of Heroin Craving." *The Journal of Neuroscience* 32.43 (2012): n. pag. Web.

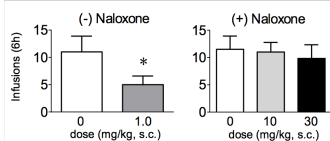
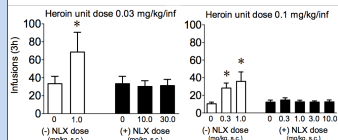
Effect of the Toll-like receptor 4 antagonist (+) naloxone and the mu opioid receptor antagonist (-) naloxone on heroin reward in rats

Obioma Ekeledo, Florence Theberge, Charles Pickens, Kenner Rice, Yavin Shaham,
Behavioral Neuroscience Branch,
NIDA/IRP/NIH/DHHS,
Baltimore, USA

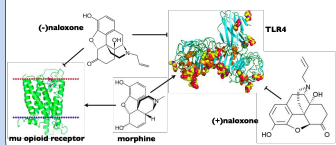


Background

- The rewarding and analgesic effects of morphine and heroin are mediated by brain mu opioid receptors and can be blocked by the preferential mu receptor agonist (+) naloxone
- Morphine (and likely heroin as well) also activates immune-function-related toll-like receptor 4 (TLR4) located on glial cells; this activation counteracts the analgesic effect of morphine
- (+) naloxone, a stereoisomer of (-) naloxone, has been recently identified as a selective antagonist of TLR4 receptors
- Northcutt et al. found that (+) naloxone prevents morphine-induced reward in the conditioned place preference (CPP) procedure
- In contrast, we found that (+) naloxone had no effect on intravenous heroin self-administration (see figures below)
- Here, we determined whether (+) naloxone is involved in heroin reward in the CPP procedure.



Actions of (+) naloxone, (-) naloxone and morphine on mu opiate receptors and TLR4 receptors



Experimental Procedures



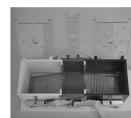
- Habituation**
•1 day, 15-min sessions
- Conditioning**
•8 days, 30-min sessions, 2 groups
•Each day given injection (s.c.) and confined to one of the two chambers
•Given free access to two distinct chambers to test for innate preferences
- Test**
•1 day, 15-min session
•Given free access to two distinct chambers to test for CPP

CPP Apparatus

•3 compartments differing by:

- Floor texture
- Wall color
- Luminosity

•Floor sensors placed throughout each compartment
•Connected to computer for data analysis
•Manually retractable doors

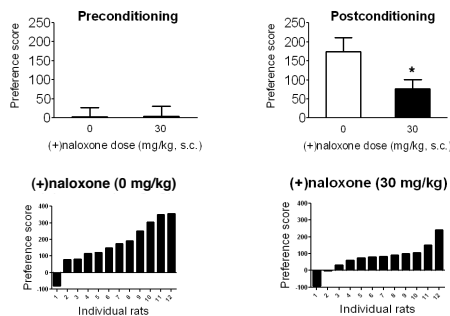


Example of conditioning pairing

Heroin (0.25 mg/kg)	Day 1		Day2	
	Heroin	Saline	Saline	Heroin
Heroin (0.25 mg/kg) + (+) naloxone (30.0 mg/kg)	Heroin (+) naloxone	Saline vehicle	Saline vehicle	Heroin (+) naloxone

Results

Pretreatment with (+) naloxne (30 mg/kg, s.c.) attenuated heroin-induced CPP



Conclusions

- (+) naloxone had no effect on heroin self-administration under fixed ratio 1 or progressive ratio reinforcement schedule.
- (+) naloxone decreased heroin-induced CPP. This result is in agreement with the data of Northcutt et al. with morphine-induced CPP.
- We currently assess the effect of (+) naloxone alone on conditioned place preference/aversion to rule out that its effect on heroin-induced CPP is due to non-specific aversive effects of the drug.

Reference

- Nortcutt et al SfN abstract 2010
- Hutchinson MR et al ScientificWorldJournal 2007; 7:98-111

Acknowledgement

- This work was supported by NIDA IRP.

Construction of odor and fluid delivery system for *in vivo* electrophysiology in behaving rats

MF Carroll, AB Kawa, AM Mirenzi, SZ Bacharach, DJ Calu
Behavioral Neuroscience Branch, NIDA/IRP/NIH, Baltimore, MD, U.S.A.

Background

- Purpose: Construct four odor/fluid delivery systems for behavioral electrophysiology studies in rats
- Method:
 - Odor cartridge construction: Air flow system assembly, solenoid wiring for independent manipulation of odor delivery.
 - Fluid system construction: fluid system assembly, solenoid wiring
 - Relay boards: wiring to power supply, wiring to odor and fluid components
- Future directions: Use the odor/fluid delivery system to probe learning about changing reward value through the use of multiple odors signaling for varying degrees of reward

Odor Cartridges

AV source and vacuum line, Side view of air flow panel, Air flow meter assembly, Tubing supplying air to odor cartridge, Top view of odor cartridge before wiring solenoids, Side view of odor cartridge, Wiring solenoids to 25-pin connector input from relay control, Solenoid wiring and air flow input, One-way valves control air/odor flow delivery to rat interface, Manifold that connects odor cartridge with rat interface

Fluid Delivery

Solenoid panel for fluid delivery, Odor and fluid input on backside of rat interface

Relay Boards

Output relays control odor and fluid delivery. Input relays record location and behavior of rat, Wiring of relays for control of odor delivery

Rat Interface and Final Product

Odor port, Photo-beam detector, Fluid well, Rat box/interface, Fluid delivery, Odor cartridge, Side view of rat box, Air flow panel, Relay board, Front view of rat box/interface

Blocking and unblocking procedure

Training - 2 weeks

Compound Conditioning - 2 days

Probe test - 1 day

How long do rats stay in the well on probe trials (extinction-no reward)?

expected reward all rats

Condition	Time spent in well (ms)
blocked	~3300
upshift	~3700
downshift	~2600

p = 0.06 (trend)
* p < 0.05 (significant)

Qualities of an award-winning poster

- Visually appealing & readable
- Organized & flows well
- Clear figures, attractive pictures
- Minimal text in bullets, white space
- Presented clearly & with enthusiasm

And remember . . .

Posters are visual &
less is best!

